Discover Applied Sciences

RESEARCH Open Access

Phytochemical profiling and in silico prediction of interactions between *Artemisia afra* Jacq. ex-Wild, *Catharanthus roseus* (L.) G. Don and CYP2B6 enzyme

Emma T. Nghilokwa[1], Jacobus P. Petzer[2], Wihan Pheiffer[1], Ibrahim Z. Hassan[3] and Rose K. Hayeshi[1*]

*Correspondence:
Rose K. Hayeshi
Rose.Hayeshi@nwu.ac.za
[1]DSI/NWU Preclinical Drug Development Platform, Faculty of Health Sciences, North-West University, Potchefstroom 2531, South Africa
[2]Centre of Excellence for Pharmaceutical Sciences, Faculty of Health Sciences, North-West University, Potchefstroom 2531, South Africa
[3]Department of Paraclinical Sciences, Faculty of Veterinary Science, University of Pretoria, Pretoria 0110, South Africa

Abstract

Understanding herb-drug interactions is important due to the increasing use of herbal medicines alongside conventional drugs. These interactions can alter the pharmacokinetic properties of drugs, potentially causing subtherapeutic effects or adverse reactions. A*rtemisia afra and Catharanthus roseus*, two traditional African plants used separately to treat malaria, are rich in phytochemicals and may be co-administered with the antimalarial drug artemether. This study aimed to identify the phytochemical compounds present in the aqueous extracts of *A. afra* and *C. roseus*, and to use in silico methods to predict the potential of these phytochemicals to inhibit CYP2B6, the enzyme that metabolises artemether. Analysis of the aqueous extracts using UHPLC-QTOF-MS identified a diverse array of phytochemicals in both plants. Potential CYP2B6 inhibitors were identified by docking the phytochemicals into the enzyme's active site using Discovery Studio software. This in silico method was validated against three metrics: root mean square deviation, enrichment factor, and receiver operating characteristic. Three docking algorithms (LibDock, LigandFit, and CDOCKER) with native scoring functions and ten additional scoring functions were assessed. The LibDock/Ludi 3 combination most effectively distinguished active inhibitors. Multiple compounds, including acacetin, isoscopoletin, and scopoletin, found in *A. afra* demonstrated strong binding affinities to the active site of CYP2B6, suggesting that phytochemicals from *A. afra* could inhibit CYP2B6-mediated metabolism, potentially affecting the pharmacokinetic profiles of co-administered substrate drugs. Such inhibition could lead to increased drug plasma concentrations, increased levels of toxicity, or reduced therapeutic efficacy, underscoring a clinically relevant risk for herb-drug interactions in populations using these herbal remedies.

Highlights

- Prominent phytochemicals in extracts of *Artemisia afra* and *Catharanthus roseus* identified by UHPLC-QTOF-MS.
- A structure-based in silico method was validated and used for molecular docking of phytochemicals identified.

- *Artemisia afra* and *Catharanthus roseus* are rich in bioactive compounds; however, only *A. afra* phytochemicals successfully interacted with the target ligand, CYP2B6.

Keywords *Catharanthus roseus*, *Artemisia afra*, In silico, CYP2B6, Computation, Herb–drug interactions

1 Introduction

African traditional medicine, deeply rooted in diverse cultural beliefs and practices, remains an important healthcare resource across the continent. With its vast biodiversity, Africa harbours a wealth of medicinal plants used to treat a range of ailments, including malaria, diabetes, and infectious diseases [1, 3, 35, 56]. Among these, *Artemisia afra* and *Catharanthus roseus* stand out as widely used plants, traditionally employed to treat malaria and other conditions [17, 56].

Given the widespread use of traditional plant-based remedies alongside modern pharmaceuticals, understanding herb-drug interactions (HDIs) has become crucial. HDIs occur when herbal compounds affect the pharmacokinetics of conventional drugs, including absorption, distribution, metabolism, or excretion, thereby potentially altering drug efficacy and safety [22, 40]. In many African communities, limited access to modern healthcare and economic factors increase reliance on herbal medicines, raising the likelihood of concurrent use with prescription drugs and the risk of clinically significant HDIs [10, 35].

Cytochrome P450 3B6 (CYP2B6), an isoform of the cytochrome P450 (CYP) enzyme family, plays an essential role in hepatic drug metabolism [15, 36, 39]. Critically, CYP2B6 metabolizes the antimalarial drug artemether, as well as key antiretroviral drugs such as efavirenz and nevirapine, all cornerstones of treatment against malaria and HIV/AIDS in sub-Saharan Africa, where the disease burden is significant [14, 18, 28, 39, 62–66]. Genetic polymorphisms in CYP2B6 can alter enzyme function, resulting in variability in drug metabolism that influences therapeutic outcomes and susceptibility to adverse drug reactions [15, 19, 55].

The inhibition of CYPs by herbal constituents can have a clinically significant impact by altering the pharmacokinetic profiles of drugs metabolised by these enzymes. For example, CYP2B6 inhibitors may reduce the metabolic clearance of antimalarials and antiretrovirals leading to increased plasma concentrations, prolonged half-life, and increased risk of toxicity or adverse effects. Conversely, inhibited metabolism can impair the production of active metabolites necessary for drug efficacy in some cases, potentially causing therapeutic failure. Therefore, CYP inhibition is central to understanding the mechanisms of HDIs, as it directly affects drug absorption and metabolism, which are critical pharmacokinetic properties that determine drug levels, duration of action, and safety [18, 26, 28, 55].

Given that CYP2B6 metabolises the antimalarial drug artemether and that *Artemisia afra* and *Catharanthus roseus* are traditionally used for the treatment of malaria, this study aimed to investigate the potential inhibitory effects of phytochemicals from *A. afra* and *C. roseus* on CYP2B6 using in silico molecular docking. This computational approach allows rapid and cost-effective prediction of molecular interactions between herbal compounds and the CYP2B6 enzyme, serving as an important screening tool to anticipate possible HDIs before expensive and time-consuming laboratory or clinical

studies [12, 21, 48]. It is complementary to laboratory experiments and animal testing [8, 44, 45, 57]. Moreover, it enables the exploration of diverse interaction scenarios, hypothesis generation, and optimization, offering a versatile and efficient way to predict herb-drug interactions [7, 32, 38, 51, 60].

While the role of CYP2B6 in metabolising synthetic drugs is well-studied, its interaction with phytochemicals from indigenous African medicinal plants, among them *A. afra* and *C. roseus* remains underexplored, highlighting the novelty and clinical relevance of this research.

2 Materials and methods

Specimens of *Artemisia afra* and *Catharanthus roseus* were acquired from the Botanical Garden of the North-West University (NWU), Potchefstroom, South Africa. Post-preparation, the herbarium specimens bearing the specimen numbers PU0016058 and PUC0016057 were transferred to the A.P Goossens Herbarium at NWU.

2.1 Preparation of extracts from Artemisia afra and Catharanthus roseus

Leaves and twigs of *A. afra* and leaves of *C. roseus* were individually manually harvested and subjected to air drying on a benchtop at room temperature for 14 days. The plant materials were finely ground individually using an electric grinder (D & A Health, Nutrition blender). A 1:10 ratio mixture was prepared from each plant by combining 10 g of the plant material with 100 mL of water from a study [2] with some modifications. The sample was heated at an escalating temperature, starting at 50 °C and sequentially increasing to 70 °C, 100 °C, 150 °C, and ultimately 200 °C for 45 min. The resulting concoction was filtered using Whatman Grade 1 filtration paper (Fisher Scientific, Sigma-Aldrich, South Africa), and the filtrates were frozen at -20 °C for 24 h, subsequently, they were lyophilised with a Lab Vacuum Freeze Dryer with High-Efficiency vacuum pump (SPS Scientific, Gardiner, NY, USA). The lyophilised extracts were stored in a desiccator at – 20 ℃ until use.

2.2 UHPLC-QTOF-MS analytical method for Artemisia afra and Catharanthus roseus

To identify the phytochemicals from the aqueous extracts of *A. afra and C. roseus* individually, UHPLC-QTOF-MS was used. Individual analyses were conducted on a Waters Acquity I Class Ultra Performance Liquid Chromatographic (UPLC) system equipped with a PDA detector. The UPLC separations were performed using an Acquity UPLC BEH C18 column (150 mm × 2.1 mm, i.d., 1.7 µm particle size), maintained at 40 °C with modifications based on [29, 43, 58]. The UPLC-MS analysis of *A. afra* was performed using a mobile phase consisting of 0.1% formic acid in water (solvent A) and acetonitrile (solvent B), with a gradient elution at a flow rate of 0.35 mL/min. The gradient started at 80% A and 20% B for 0.5 min, increased to 40% A and 60% B over 13 min, then ramped to 100% B in 2.5 min, held for 0.5 min, before returning to initial conditions for equilibration, with a total runtime of 18 min. Mass spectrometric detection was carried out in negative electrospray ionization mode Fig. 1. Nitrogen served as the desolvation gas at a flow rate of 600 L/hr with the desolvation temperature set at 350 °C and source temperature at 100 °C. The capillary voltage was maintained at 2500 V and the cone voltage at 40 V, with data acquired over an m/z range of 100 to 1500. The LockSpray™ interface was

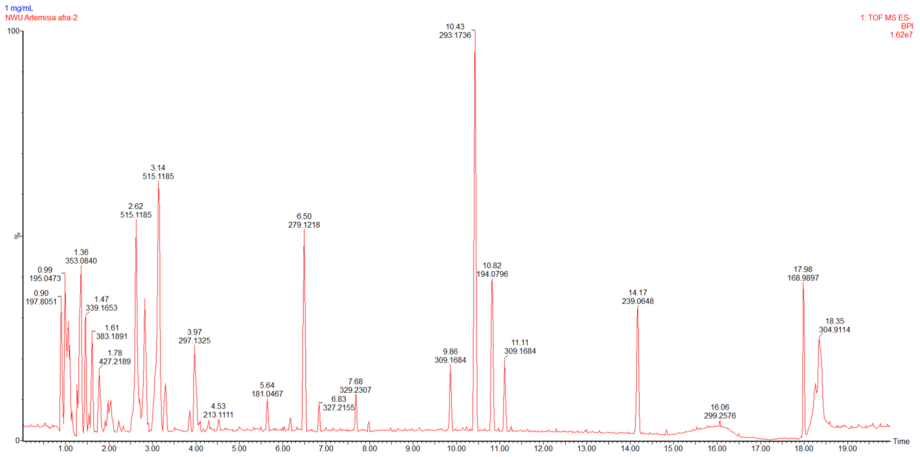

Fig. 1 Chromatogram of UHPLC-QTOF-MS of aqueous extracts of *Artemisia afra*, showing the peaks of different identified phytochemical compounds

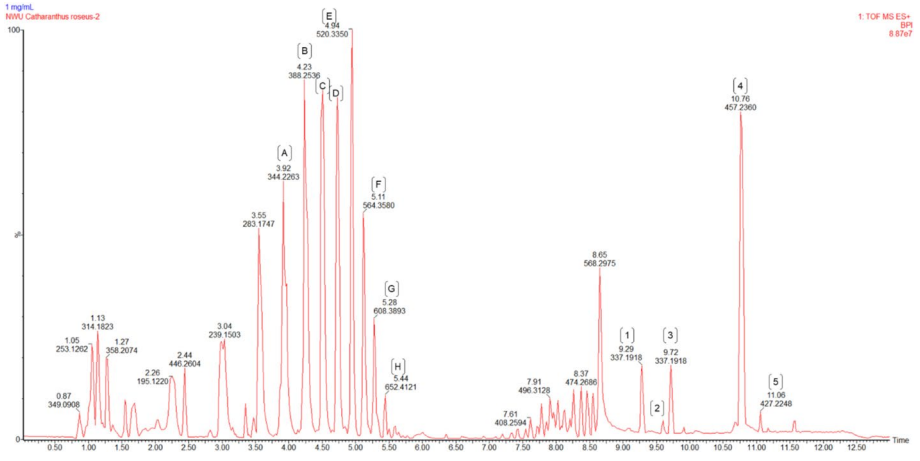

Fig. 2 Chromatogram of UHPLC-QTOF-MS of aqueous extracts of *Catharanthus roseus*, showing the peaks of different identified phytochemical compounds

employed throughout to ensure mass accuracy and reproducibility. Compound identification was based on mass accuracy and processed using MassLynx 4.2 software.

The UPLC-MS analysis of *C. roseus* utilised a mobile phase of 0.1% formic acid in water (solvent A) and acetonitrile (solvent B) with a gradient elution at 0.3 mL/min, starting at 90% A and 10% B for 1 min, shifting to 40% A and 60% B over 8 min, then to 20% A and 80% B in 2 min, before returning to initial conditions with a total runtime of 13 min. Mass spectrometry was performed in positive electrospray ionization mode using nitrogen as the desolvation gas at 600 L/hr and a desolvation temperature of 400 °C, with a source temperature of 100 °C. The capillary voltage was set at 3300 V and the cone voltage at 40 V, acquiring data across an m/z range of 100 to 1500 Fig. 2. Compound identification was ensured by applying the LockSpray™ interface for mass accuracy and reproducibility, with data processed using MassLynx 4.2 software. This section was outsourced to Tshwane University of Technology, Pretoria, South Africa. Data collection was performed between 100 and 1500 m/z using the LockSpray™ interface for accuracy and reproducibility during acquisition.

2.3 In silico molecular docking method validation

A structure-based in silico method was employed to identify phytochemicals from *A. afra* and *C. roseus* that might possess the potential to inhibit the CYP2B6 enzyme. For this purpose, the Discovery Studio 3.1 life sciences molecular modelling software was used (Accelrys Inc., San Diego, USA). The reported crystal structures of the CYP2B6 enzyme in complex with 4-(4-chlorophenyl) imidazole Protein Data Bank Identification (PDB ID: 3IBD) served as protein model [16] Based on the good resolution (2 Å) of this structure, it was deemed a suitable model for the in silico studies. Various docking algorithms and scoring functions were first evaluated to find the combination that best identified active inhibitors within a database of active and decoy compounds. This validation step evaluated three metrics: the Root Mean Square Deviation (RMSD), Enrichment Factor (EF), and Receiver Operating Characteristic (ROC) curve. RMSD measured the ability of each docking/scoring combination to accurately redock thirteen chosen high-resolution co-crystallised ligands back onto the active site of the selected target protein CYP2B6. The EF and ROC measured the ability of each combination to identify active inhibitors (n = 13) from among a set of 1001 decoy compounds. Three docking algorithms (LibDock, LigandFit, CDOCKER) with their native scoring functions and ten additional scoring functions were evaluated, as recently reported [48].

2.3.1 Target preparation and molecular docking

Target protein preparation and molecular docking were done according to Ibrahim et al. [21] and Shaw et al. [48]. The CYP2B6 protein model was prepared in Discovery Studio. The protein was typed with the Momany and Rone CHARMm forcefield. The ionisation states and pKa values of the ionisable amino acids were calculated, and the model was protonated at pH 7.4. A fixed-atom constraint was applied to the backbone, and the protein was minimised using the Smart Minimizer algorithm, with the maximum steps set to 50,000. The implicit Generalized Born with Molecular Volume (GBMV) solvent model was employed during minimisation without the use of SHAKE constraints. The co-crystallised ligand and water molecules were removed from the protein, and the active site was identified from an analysis of the cavities that are present in the protein [21, 48].

Thereafter, the ligands that were docked were constructed in Discovery Studio, and their geometries were briefly optimised using a Dreiding-like forcefield (5000 iterations) [21, 48]. The structures of the ligands were prepared with the Prepare Ligands protocol. Subsequently, docking was performed with the CDOCKER, LibDock, and LigandFit algorithms, in which each employed a native scoring function: CDOCKER Energy, LibDock Score and Dock Score, respectively. The docked solutions were rescored with the LigScore 1 & 2, PLP1, PLP2, Jain, PMF, PMF04 and Ludi 1, 2 & 3 scoring functions[21, 48]. For all three docking algorithms, the default settings were applied. For CDOCKER, ten random conformations were generated in full potential mode and with a heating target temperature of 700 K. For LibDock, the conformation method was set to BEST. In situ minimisation of the solutions was not carried out [21, 48].

2.3.2 Root mean square deviation

The co-crystallised ligands found in the CYP2B6 shown in Table 1 were docked into the selected protein model (PDB ID: 3IBD) using the three selected docking algorithms. The

Table 1 The reported crystal structures of CYP2B6 were considered for this study

Allocated number	PDB code	Resolution (Å)
1	3IBD [16]	2.00
2	3QOA [47]	2.10
3	3QU8 [47]	2.80
4	3UA5 [47]	2.80
5	4I91 [47]	2.00
6	4RQL [49]	2.10
7	4RRT [49]	2.20
8	4ZV8 [33]	2.24
9	5UAP [46]	2.03
10	5UDA [46]	1.93
11	5UEC [46]	2.27
12	5UFG [46]	1.76
13	5WBG [50]	2.99

Structure 3IBD was selected as protein model for the in silico studies, while co-crystallised ligands present in these structures were used to calculate RMSD values during the assessment of the ability of the docking/scoring function to correctly orientate ligands within the binding site

Table 2 The structures of the 14 active compounds [53, 54] that were selected to evaluate combinations of docking algorithms and scoring functions for the ability to select active CYP2B6 inhibitors from decoy compounds

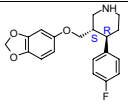 Paroxetine IC_{50} /K_i = 1.6 µM	 2-Phenyl-2-(1-piperidinyl)propane IC_{50} /K_i = 1.2 µM	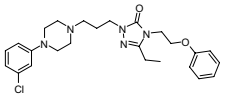 Nefazodone IC_{50} /K_i = 1.6 µM	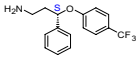 Norfluoxetine IC_{50} /K_i = 4.2 µM	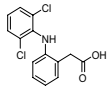 Diclofenac IC_{50} /K_m = 1.5-3 µM
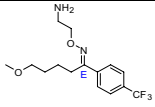 Fluvoxamine IC_{50} /K_i = 6.1 µM	 4-(4-Chlorophenyl)imidazole IC_{50} /K_i = 0.27 µM	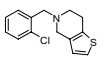 Ticlopidine IC_{50} /K_i = 0.2-0.8 µM	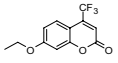 7-Ethoxy-4-trifluoromethylcoumarin (7-EFC) IC_{50} /K_m = 1.7 µM	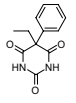 Phenobarbital IC_{50} /K_m = 7.2 µM
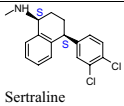 Sertraline IC_{50} /K_i = 3.2 µM K_m = 31 µM	 4-Benzylpyridine IC_{50} /K_i = 3.5 µM	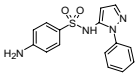 Sulfaphenazole IC_{50} /K_i = 0.3 ± 0.1 µM	 (1S,5R)-2-(Bromomethyl)-6,6-dimethyl bicyclo[3.1.1]hept-2-ene IC_{50} /K_i = 1.5 µM	

solutions were rescored with the scoring functions, and the root-mean-square deviation (RMSD) of the heavy atoms from the position of the co-crystallised ligand was calculated within Discovery Studio. The success rate (as described in Eq. 1) was established from the ligands that displayed an RMSD value of ≤ 2.5 Å [9, 48].

$$Success\,rate = \left(Number\,of\,ligands \leq 2.5\text{Å} / Total\,number\,of\,ligands\right) \times 100 \quad (1)$$

2.3.3 Datasets of active and decoy compounds

Thirteen (13) (Table 1) compounds known substrates or inhibitors of CYP2B6 were selected from the literature [53, 54]. These compounds represent the active dataset, and their molecular structures are given in Table 2. The decoy compounds employed in this study were sourced from the directory of useful decoys enhanced (DUD-E) database [37, 48]. The 13 active compounds were submitted to the DUD-E search algorithm, resulting

in the generation of 50 to 100 decoy compounds for each active compound. Subsequently, 987 decoy compounds were retrieved from the DUD-E database and prepared for the docking simulations as described above. A second decoy dataset (n = 1001) was obtained from Schrödinger (New York, USA).

2.3.4 Enrichment factor (EF)

The dataset employed in this study included 987 decoy compounds from the DUD-E decoy database and 999 compounds from the Schrödinger database. The 13 active compounds were added to these datasets to yield final datasets of 1001 and 1013 compounds, respectively. Subsequently, these datasets were docked into the selected protein model (PDB ID: 3IBD) using the CDOCKER, LibDock, and LigandFit docking algorithms. Following the docking simulations, the solutions were rescored with the selected scoring functions. Equation 2 was used to calculate the Enrichment Factor (EF) using Microsoft Excel for Microsoft Office 365 (Microsoft, United States). EF represents the ratio of active compounds within a specified percentage (e.g., 10%) of the database to the entire database [31, 34, 48, 61].

$$EF = (Hits_{sel}/Hits_{tot}) \times (NC_{tot}/NC_{sel}) \quad (2)$$

$Hits_{sel}$ refers to the number of active compounds within the designated percentage (e.g., 10%) of the dataset. $Hits_{tot}$ indicates the total number of active compounds (n = 13) present in the dataset. NC_{tot} represents the total number of compounds (active and decoy) in the entire dataset, while NC_{sel} represents the number of compounds (active and decoy) in the designated percentage of the dataset [31, 34, 48, 61].

2.3.5 Receiver operating characteristic (ROC)

The datasets used for calculating the EF were also used to evaluate the ROC. The ROC analysis was conducted using SPSS Statistics version 27 for Windows (IBM, United States). The ROC assesses the ability of the combination of the docking and scoring function in discriminating between active compounds and decoys [5, 30]. The efficacy is assessed with the area under the curve (AUC) [5, 30]. The AUC serves as a measure of how effectively a scoring function prioritizes active compounds over decoys and should be evaluated as follows: AUC values from 1.0 to 0.9 indicate an excellent performance, while those between 0.9 and 0.8 are considered good, 0.8 to 0.7 are classified as fair, values from 0.7 to 0.5 are deemed poor, and an AUC below 0.5 signifies failure [48].

2.3.6 Screening for potential binding to CYP2B6

To evaluate the potential of plant components from *A. afra* and *C. roseus* to inhibit CYP2B6, the compounds reported to be present in these plants were drawn in Discovery Studio, and their geometries were optimized and prepared for the docking simulations as described above. The list of the plant components is given in Table 3 which were obtained from literature [4, 25, 27, 41, 58]. The selected compounds were chosen due to their status as the most abundant phytochemicals identified in *A. afra* and *C. roseus* plants in Southern Africa. The components were docked into the active site of the CYP2B6 protein model (PDB ID: 3IBD) with LibDock and the resulting solutions were rescored with Ludi 3, as the LibDock/Ludi3 was the combination that best differentiated between active and decoy compounds. The components with the highest Ludi 3 scores

Table 3 Literature based prominent phytochemicals in *Artemisia afra* and *Catharanthus roseus* in Southern Africa

Phytochemicals in *Artemisia afra*	Phytochemicals in *Catharanthus roseus*
L- (-)-Camphor	Ajmaline
Camphene	Yohimbine
1,8-Cineole	Vindesine
Scopoletin	Ajmalicine
Isoscopoletin	Serpentine
Scopolin	Vinblastine
Artemisia ketone	Vincristine
Santolina alcohol	(-)-Vindoline
(+)-β-Thujone	Vinpocetin
Acacetin	(-)-Reserpine
Chrysoeriol	
3,5-O-dicaffeoylquinic acid	
Rutin	

are most likely to bind to CYP2B6, and these scores were compared to those of known inhibitors.

3 Results and discussion

3.1 UHPLC-QTOF-MS chemical analysis of Artemisia afra and Catharanthus roseus aqueous extracts

Characterising the chemical profiles of *A. afra* and *C. roseus* using UHPLC-QTOF-MS analysis provided valuable insights into their phytochemical compositions and bioactive compounds. Some of the bioactive compounds identified in our study differed from those commonly reported in the literature [41, 59]. Specifically, in addition to dicaffeoylquinic acids and chlorogenic acid, our UHPLC-QTOF-MS analysis revealed the presence of tehranolide, hydroxyartemisin, artemisitene, and gmelinin compounds that are either rarely reported or absent in previous studies on *A. afra* from other regions [13, 24, 41]. For instance, tehranolide and hydroxyartemisin have not been detected in *A. afra* samples collected from regions such as Bronkhorstspruit or Potchefstroom. This variation may be attributed to differences in environmental conditions, soil composition, and genetic diversity across geographic locations [24, 41]. Bioactive compounds, such as catharanthine, tabersonine, vindolinine, vindoline, and vindolicine, were detected in *C. roseus* aqueous extracts through UHPLC-QTOF-MS analysis (Table 4). Similar bioactive compounds were reported in the same plant extracts [20, 23, 42], which were collected at different locations. Our literature review and UHPLC-QTOF-MS analysis revealed no evidence that any bioactive compounds from *C. roseus* interact with the CYP2B6 protein. The absence of interaction in silico suggests that the plant's bioactive compounds may not significantly inhibit CYP2B6 activity, which is important for some antimalarials and anti-HIV drug metabolism. This could imply a lower risk of herb-drug interactions involving this specific enzyme.

3.2 In silico molecular docking method validation

An in silico structure-based approach was followed to predict if compounds from *A. afra* and *C. roseus* might possess the ability to inhibit CYP2B6. Different docking algorithms and scoring functions were first evaluated to identify which combinations can discern known CYP2B6 inhibitors from inactive compounds in a library of compounds

Table 4 Phytochemicals identified in an *Artemisia afra* and *Catharanthus roseus* aqueous extracts by UHPLC-QTOF-MS

Artemisia afra						*Catharanthus roseus*					
Peak #	**Retention time (min)**	***m/z* ratio**	**(Error) ppm**	**Molecular formula**	**Putative identification**	**Peak #**	**Retention time (min)**	***m/z* ratio**	**(Error) ppm**	**Molecular formula**	**Putative identification**
1	1.09	515.1183	− 1.0	$C_{25}H_{24}O_{12}$	Dicaaffeoylquinic acid (**I**)	**1**	9.29	337.1918	0.6	$C_{21}H_{24}N_2O_2$	Catharanthine Tabersonine Vindolinine
2	1.36	353.0840	− 9.3	$C_{16}H_{18}O_9$	Chlorogenic acid	**2**	9.60	337.1918	0.6	$C_{21}H_{24}N_2O_2$	Catharanthine Tabersonine Vindolinine
3	1.47	339.1655	− 0.6	$C_{14}H_{28}O_9$	_	**3**	9.79	337.1918	0.6	$C_{21}H_{24}N_2O_2$	Catharanthine Tabersonine Vindolinine
4	2.63	515.1183	− 1.0	$C_{25}H_{24}O_{12}$	Dicaaffeoylquinic acid (**II**)	**4**	10.76	457.2360	4.4	$C_{25}H_{32}N_2O_6$	Vindoline
5	2.82	515.1185	− 1.0	$C_{25}H_{24}O_{12}$	Dicaaffeoylquinic acid (**III**)	**5**	11.06	427.2248	3.5	$C_{24}H_{30}N_2O_5$	Vindolicine
6	3.15	515.1185	− 1.0	$C_{25}H_{24}O_{12}$	Dicaaffeoylquinic acid (**IV**)						
7	3.98	297.1338	− 4.4	$C_{15}H_{22}O_6$	Tehranolide/Hydroxyartemisin						
8	6.52	279.1218	15.8	$C_{15}H_{20}O_5$	Artemisitene						
9	10.43	293.1736	− 5.8	$C_{17}H_{26}O_4$	Gmelinin						

that contains both inactive (decoy compounds) and active compounds. This validation step was done using three metrics: the RMSD, EF, and the ROC. The RMSD determines which of the docking/scoring combinations can correctly predict the binding orientation of known inhibitors in the active site. The EF and ROC determine if the docking/scoring combinations can identify active compounds in a library that contains both active and decoy compounds. This validation is essential and identifies the best docking algorithm and scoring function to predict whether compounds (e.g., phytochemicals from *A. afra* and *C. roseus*) might act as CYP2B6 inhibitors.

This study selected the X-ray crystal structure of the human CYP2B6 enzyme with 4-(4-chlorophenyl) imidazole bound to the active site (PDB ID: 3IBD) for the docking study. The molecular modelling software, Discovery Studio, was used for the docking simulations. Three docking algorithms were evaluated (CDOCKER, LibDock, LigandFit), each possessing its native scoring function, namely CDOCKER Energy, LibDock Score, and Dock Score, respectively. An additional ten scoring functions (LigScore 1, LigScore 2, PLP1, PLP2, Jain, PMF, PMF04, and Ludi 1, 2 & 3) were also evaluated for each docking algorithm. The docking algorithm proposes potential orientations/poses of the ligand within a binding site, while the scoring function identifies the orientation that is most probable based on higher binding affinity and more productive interactions with the protein target [11, 37].

3.2.1 Root mean square deviation

This study evaluated the accuracy with which the three docking algorithms were able to redock 13 ligands that have been co-crystallised with the CYP2B6 enzyme into the active site of the enzyme, and the ability of the scoring functions to rank the correct orientations. Tables 5 and 6 report the RMSD between the docked orientations and the positions of the ligands in the co-crystallised structures. An RMSD ≤ 2.5 Å indicates that a docking algorithm has successfully reproduced the crystallographic pose for a known ligand. The results showed that CDOCKER and LibDock had 33 and 22% success rates (RMSD ≤ 2.5 Å) when scoring the poses with the native scoring functions, while LigandFit was unable to dock the ligands into the CYP2B6 active site. For this analysis, the RMSD of the first-ranked pose was used. The co-crystallised ligands present in the structures of 3QU8, 3UA5, 5UFG and 5WBG could not be docked with LibDock, while the structure present in 3UA5 could not be docked with CDOCKER. For CDOCKER, the LigScore 2 function yielded the best success rate (42%) while LigScore 1 and PMF04 had the highest success rate when combined with LibDock (33%). Interestingly, LibDock had a 78% success rate in reproducing the crystallographic orientation irrespective of the rank of the best pose. This shows that LibDock could correctly reproduce the orientation of the ligand within the total number of poses generated. Although LibDock demonstrates the ability to find solutions where the ligands are correctly docked with respect to binding orientation, no scoring function had a high success rate in identifying orientations with RMSD ≤ 2.5 Å. The implications of this in silico structure-based approach in predicting herb-drug interactions are useful. This process, which employed the CYP2B6 enzyme's crystal structure (PDB:3IBD) in Table 1, demonstrated that LibDock could reproduce ligand orientations with a high success rate, despite the lower accuracy of scoring functions in identifying correct poses in Tables 5 and 6. This approach can streamline the identification of active compounds from decoy compounds. The selection

Table 5 Root Mean Square Deviation values obtained after docking with *CDOCKER* and scoring the various poses with selected scoring functions

PDB Code	Best pose (pose rank)	Native—1st	LigScore 1—1st (pose rank)	LigScore 2—1st (pose rank)	PLP1—1st (pose rank)	PLP2—1st (pose rank)	Jain—1st (pose rank)	PMF—1st (pose rank)	PMF4—1st (pose rank)	Ludi 1—1st (pose rank)	Ludi 2—1st (pose rank)	Ludi 3—1st (pose rank)
3IBD	1.1 (10)	1.2	1.2 (7)	1.2 (7)	1.2 (2)	1.2 (2)	1.2 (7)	1.2 (3)	1.1 (4)	1.2 (5)	1.2 (5)	1.2 (5)
3QOA	2.6 (8)	2.6	2.8 (5)	2.7 (10)	2.8 (9)	2.8 (9)	2.6 (1)	2.6 (8)	2.6 (7)	2.6 (1)	2.8 (4)	2.8 (4)
3QU8	1.8 (8)	2.0	1.9 (6)	2.0 (9)	1.9 (10)	1.9 (6)	1.8 (5)	1.9 (6)	1.8 (8)	1.8 (5)	1.9 (2)	1.9 (10)
3UA5	–	–	–	–	–	–	–	–	–	–	–	–
4I91	2.1 (2)	2.1	2.1 (1)	2.1 (1)	2.1 (1)	2.1 (1)	4.4 (9)	2.8 (7)	4.4 (8)	2.8 (7)	4.4 (9)	4.4 (9)
4RQL	3.8 (10)	4.0	3.9 (6)	3.9 (6)	3.9 (2)	4.0 (4)	3.8 (10)	3.9 (5)	3.9 (5)	4.0 (1)	4.0 (1)	4.0 (4)
4RRT	3.7 (7)	3.8	3.8 (2)	3.8 (2)	3.7 (6)	3.8 (2)	3.9 (3)	3.9 (4)	3.8 (2)	3.8 (2)	3.8 (2)	3.9 (3)
4ZV8	1.9 (2)	1.9	1.9 (1)	1.9 (1)	1.9 (1)	1.9 (1)	4.3 (9)	2.7 (7)	4.3 (8)	2.7 (7)	4.3 (9)	4.3 (9)
5UAP	2.7 (2)	3.2	3.2 (1)	3.2 (1)	3.2 (1)	3.1 (7)	2.7 (2)	2.7 (3)	3.1 (8)	2.7 (2)	3.1 (5)	2.7 (4)
5UDA	2.2 (7)	2.8	2.8 (1)	2.3 (6)	2.9 (3)	2.9 (3)	2.8 (1)	3.6 (2)	3.6 (2)	2.7 (8)	3.6 (2)	3.6 (2)
5UEC	2.6 (1)	2.6	2.9 (2)	2.9 (2)	4.1 (8)	4.1 (10)	2.6 (1)	4.1 (9)	4.1 (10)	2.9 (3)	2.8 (4)	4.1 (5)
5UFG	2.8 (4)	2.9	2.8 (4)	2.9 (1)	4.1 (8)	4.1 (6)	2.9 (3)	2.9 (2)	2.8 (4)	2.9 (2)	2.8 (5)	4.1 (6)
5WBG	5.1 (3)	5.1	5.1 (3)	5.1 (3)	5.1 (5)	5.1 (5)	5.2 (6)	5.2 (10)	5.1 (1)	5.1 (3)	5.2 (9)	5.2 (9)
Total	**5**	**4**	**4**	**5**	**4**	**4**	**2**	**2**	**2**	**2**	**2**	**2**
Ave. RMSD	**2.7**	**2.9**	**2.9**	**2.8**	**3.1**	**3.1**	**3.2**	**3.1**	**3.4**	**2.9**	**3.3**	**3.5**
Success rate	**42**	**33**	**33**	**42**	**33**	**33**	**17**	**17**	**17**	**17**	**17**	**17**

- No results obtained

* Number of ligands with an RMSD value < 2.5

† Percentage of ligands with and RMSD value < 2.5

‡ Native scoring function for CDOCKER (CDOCKER Energy)

of the libDock/Ludi 3 was based on the higher EF and ROC-AUC values compared to the scoring function combinations.

3.2.2 Enrichment factor and receiver operating characteristic

For calculation of the EF and ROC curve, two libraries were constructed: The first contained 14 actives as well as decoys from the DUDe database with a total number of compounds of 1001, while the second contained the 14 actives as well as decoys from the Schrödinger decoy database with a total number of compounds of 1013. This validation was carried out for LibDock only since CDOCKER would be computationally too expensive to dock larger datasets of compounds. The EF data (Tables 7) showed that LibDock combined with Ludi 3 performed best with both the DUDe (EF10%: 2.12 and 7.80) and Schrodinger decoy sets (EF10%: 2.12 and 7.80). The higher value signifies that 7.80% of the actives would be present among the top 10% compounds in a database.

When considering the area under the curve (AUC) of the ROC curves, LibDock combined with Ludi 3 again yielded the best results for both the DUDe and Schrodinger decoy sets. The AUC values were 0.782 and 0.648, respectively. The AUC measures how well a scoring function ranks actives higher than decoys and could be interpreted as fair [$1.0 \geq AUC \geq 0.9$ (excellent), $0.9 > AUC \geq 0.8$ (good), $0.8 > AUC \geq 0.7$ (fair), $0.7 > AUC \geq 0.5$ (poor) and an $AUC < 0.5$ (failure)].

The validation process found that the LibDock/Ludi 3 combination performed best at identifying active compounds. Using this combination, 23 phytochemicals that are known to be present in *A. afra* and *C. roseus* (Table 2) were docked into the protein model of CYP2B6 and the resulting poses were scored. Of the 23 phytochemicals evaluated, only these 11 could be docked by LibDock (Table 8).

Table 8 show that acacetin (897), isoscopoletin (759), and scopoletin (705) presented with high Ludi 3 scores. These scores were similar to those of the known inhibitors, ticlodipine (939), 4-benzylpyridine (851), and 4-(4-chlorophenyl) imidazole (742), which suggests that these phytochemicals might have the potential to bind to CYP2B6 (Raunio et al., 2020).

The Enrichment Factor (EF) and Receiver Operating Characteristic (ROC) analysis are useful in drug development. EF is essential for assessing the efficiency of virtual screening methods, such as molecular docking, in identifying active compounds from larger datasets. This study finds scopoletin, isoscopoletin, and acacetin with higher EF values indicating a greater probability of acting as inhibitors (Table 8, Fig. 3A–C). ROC, with AUC values closer to 1, evaluates the performance of binary classification models in distinguishing actives from decoys, demonstrating high accuracy in ranking active compounds. These findings suggest that incorporating EF and ROC analyses can enhance the process by improving the accuracy and efficiency of identifying compounds with therapeutic potential. By evaluating the docking algorithms and scoring functions, this study identified combinations that effectively discern CYP2B6 inhibitors from inactive compounds. The validation using RMSD, EF, and ROC metrics was critical in selecting the best docking algorithm and scoring function for accurate predictions (Tables 5, 6 and 7). The interaction of CYP2B6 with acacetin, isoscopoletin, and scolopetin Fig. 3 A–C underscores the enzyme's substrate selectivity and the intricate binding interactions inside its active site. The presence of Val367, which stabilizes both acacetin and scopoletin, indicates that these residues may be essential in tolerating molecules with

Table 6 Root Mean Square Deviation values obtained after docking with *LibDock* and scoring the various poses with selected scoring functions

PDB Code	Best pose (pose rank)	Native—1st	LigScore 1—1st (pose rank)	LigScore 2—1st (pose rank)	PLP1—1st (pose rank)	PLP2—1st (pose rank)	Jain—1st (pose rank)	PMF—1st (pose rank)	PMF4—1st (pose rank)	Ludi 1—1st (pose rank)	Ludi 2—1st (pose rank)	Ludi 3—1st (pose rank)
3IBD	0.7 (7)	1.2	1.2 (1)	1.2 (1)	4.6 (9)	4.6 (9)	5.5 (13)	0.9 (2)	0.9 (6)	1.2 (1)	1.0 (3)	0.9 (6)
3QOA	2.3 (4)	2.8	2.3 (4)	5.5 (8)	5.5 (8)	5.3 (9)	2.5 (5)	2.8 (11)	2.3 (4)	2.8 (2)	2.8 (2)	2.8 (6)
3QU8	–	–	–	–	–	–	–	–	–	–	–	–
3UA5	–	–	–	–	–	–	–	–	–	–	–	–
4I91	2.5 (6)	3.5	3.5 (1)	3.5 (1)	3.5 (1)	3.5 (1)	3.2 (3)	3.8 (12)	3.8 (12)	7.9 (4)	7.9 (4)	3.8 (12)
4RQL	2.1 (3)	2.6	3.8 (4)	3.8 (4)	3.8 (4)	2.6 (1)	3.1 (19)	2.8 (7)	4.2 (17)	4.1 (12)	2.9 (5)	3.5 (11)
4RRT	1.8 (15)	8.0	2.5 (11)	2.5 (11)	3.7 (2)	3.8 (3)	4.7 (38)	2.5 (11)	3.8 (3)	8.0 (1)	8.0 (1)	3.3 (6)
4ZV8	2.4 (6)	3.7	3.7 (1)	3.7 (1)	3.7 (1)	3.7 (1)	3.4 (3)	3.8 (12)	3.8 (12)	7.8 (4)	7.8 (4)	3.8 (12)
5UAP	2.7 (7)	3.2	3.6 (6)	3.6 (6)	3.2 (2)	3.2 (1)	4.3 (4)	2.7 (7)	2.7 (7)	3.2 (3)	4.3 (4)	2.7 (7)
5UDA	3.0 (1)	3.0	3.5 (3)	3.5 (3)	3.5 (3)	3.5 (3)	3.0 (1)	3.2 (5)	3.5 (3)	3.5 (3)	3.4 (4)	3.6 (2)
5UEC	2.0 (8)	2.1	2.7 (6)	2.7 (6)	2.2 (2)	2.2 (2)	2.7 (6)	2.6 (10)	2.3 (12)	2.4 (13)	4.2 (23)	3.2 (14)
5UFG	–	–	–	–	–	–	–	–	–	–	–	–
5WBG	–	–	–	–	–	–	–	–	–	–	–	–
Total	**7**	**2**	**3**	**2**	**1**	**1**	**1**	**2**	**3**	**2**	**1**	**1**
Ave. RMSD	**2.2**	**3.3**	**3.0**	**3.3**	**3.8**	**3.6**	**3.6**	**2.8**	**3.0**	**4.5**	**4.7**	**3.1**
Success rate	**78**	**22**	**33**	**22**	**11**	**11**	**11**	**22**	**33**	**22**	**11**	**11**

- No results obtained

* Number of ligands with an RMSD value < 2.5

† Percentage of ligands with an RMSD value < 2.5

‡ Native scoring function for LibDock (LibDock Score)

Table 7 Enrichment factor at 10% ($EF^{10\%}$) and ROC curve area under the curve (AUC) after docking a set of DUDe decoy compounds and a set of Schrödinger decoy compounds, that was seeded with 14 active inhibitors with LibDock (n-total = 1001, and n-total = 1013, respectively)

Scoring functions	LibDock_Score	LigScore 1	LigScore 2	PLP1	PLP2	Jain	PMF	PMF4	Ludi 1	Ludi 2	Ludi 3
DUDe decoy compounds											
Enrichment factor at 10%	2.83	1.42	0.00	2.83	2.83	0.00	2.83	2.12	1.42	0.71	2.12
ROC	0.57	0.477	0.469	0.578	0.579	0.366	0.557	0.476	0.456	0.455	0.782
Schrödinger decoy compounds											
Enrichment factor at 10%	3.55	3.55	4.26	3.55	3.55	4.97	4.97	7.80	2.84	4.97	7.80
ROC	0.44	0.507	0.595	0.462	0.476	0.534	0.609	0.71	0.456	0.522	0.648

Maximum EF = 10

ROC curve AUC values: 1—0.9 = excellent; 0.89—0.8 = good; 0.79—0.7 = fair; 0.69—0.6 = poor

analogous structural features. Simultaneously, the notable roles of Ile101 and Phe115 in stabilizing acacetin and isoscopoletin (Fig. 4) suggest a possible inclination of CYP2B6 towards drugs with particular aromatic or hydrophobic properties. The effective interaction of heme with isoscopoletin highlights the significance of heme as a cofactor in CYP450 enzymes, promoting electron transport and metabolic changes. This interaction may influence the efficiency of substrate metabolism and could be indicative of binding nuances that affect overall catalytic activity. Understanding these particular interactions helps in clarifying the mechanism of the enzyme and may direct the development of more targeted inhibitors or therapeutics aimed at modulating CYP2B6 activity.

The bioactive compounds identified in the *A. afra* aqueous extract (acacetin and isoscopoletin, scopoletin, coumarins) demonstrated good binding affinity to the target protein, CYP2B6, and could be regarded as potential inhibitors of human CYP2B6 enzyme. Notably, these compounds showed Ludi 3 scores like known inhibitors such as ticlodipine, 4-benzylpyridine, and 4-(4-chlorophenyl) imidazole. The current in silico data suggest that caution may need to be exercised when combining CYP2B6 substrate drugs with aqueous extracts from *A. afra* to avoid adverse events. In vivo validation of this data is currently underway in appropriate rodent models. The data will be able to inform the need for patients presenting for treatment at health care facilities to disclose their use of any herbal or conventional drug(s) to avoid unwanted inhibitory interactions, given that this could result in potential drug toxicity, reduced effect of the substrate drugs, or unexpected side effects [6, 52, 67].

In silico molecular docking was useful for predicting CYP2B6 protein–ligand interactions but has limitations, especially with larger molecules. Due to structural constraints, the CYP2B6 protein binding site could only accommodate small molecules. Larger molecules also had more complex structures, increasing the risk of steric clashes and reducing prediction accuracy. Furthermore, existing tools like Stitch and MetaDrug, which have machine learning and artificial intelligence capabilities, would be adequate to handle different molecular sizes and reduce the possibility of steric conflicts, which might result in inaccurate readings. Therefore, tiny ligand molecules are better suited for in silico molecular docking. Moreover, it is difficult to find possible specific targets using computational methods such as in silico molecular docking. Molecular Dynamics (MD) simulations were not performed in this work due to constraints in the available computing tools and resources. We recognise that this may limit the evaluation of

Table 8 The Ludi 3 scores of the first-ranked poses of phytochemicals from *Artemisia afra* and *Catharanthus roseus* after docking with LibDock. The scores of selected reference CYP2B6 inhibitors are also given

	***Artemisia afra* bioactive compounds**											**Reference inhibitors**		
	L-(-)-Camphor	**Camphene**	**1,8-Cineole**	**Scopoletin**	**Isoscopoletin**	**Scopolin**	**Artemisia ketone**	**Santolina alcohol**	**(+)-β-Thujone**	**Acacetin**	**Rutin**	**Ticlodipine**	**4-Benzylpyridine**	**4-(4-Chlorophenyl) imidazole**
Ludi 3 score	401	534	345	**705**	**759**	230	398	315	442	**897**	271	939	851	742

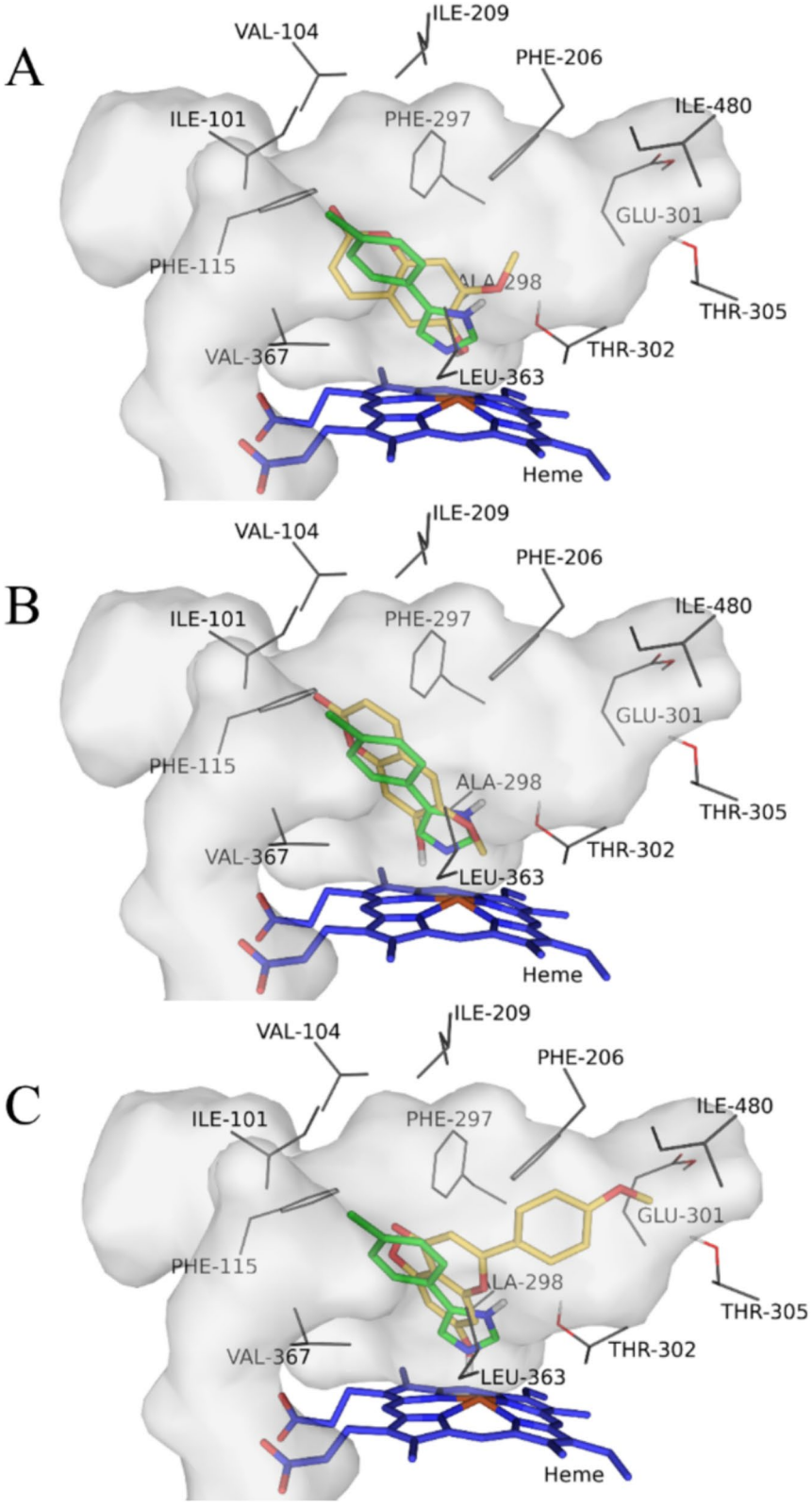

Fig. 3 The predicted binding orientations of (**A**) isoscopoletin, **B** scopoletin and **C** acacetin in the CYP2B6 active site. The orientation of 4-(4-chlorophenyl) imidazole is shown in green, haeme is shown in blue, and the natural products tested are shown in yellow. Images generated using PyMOL

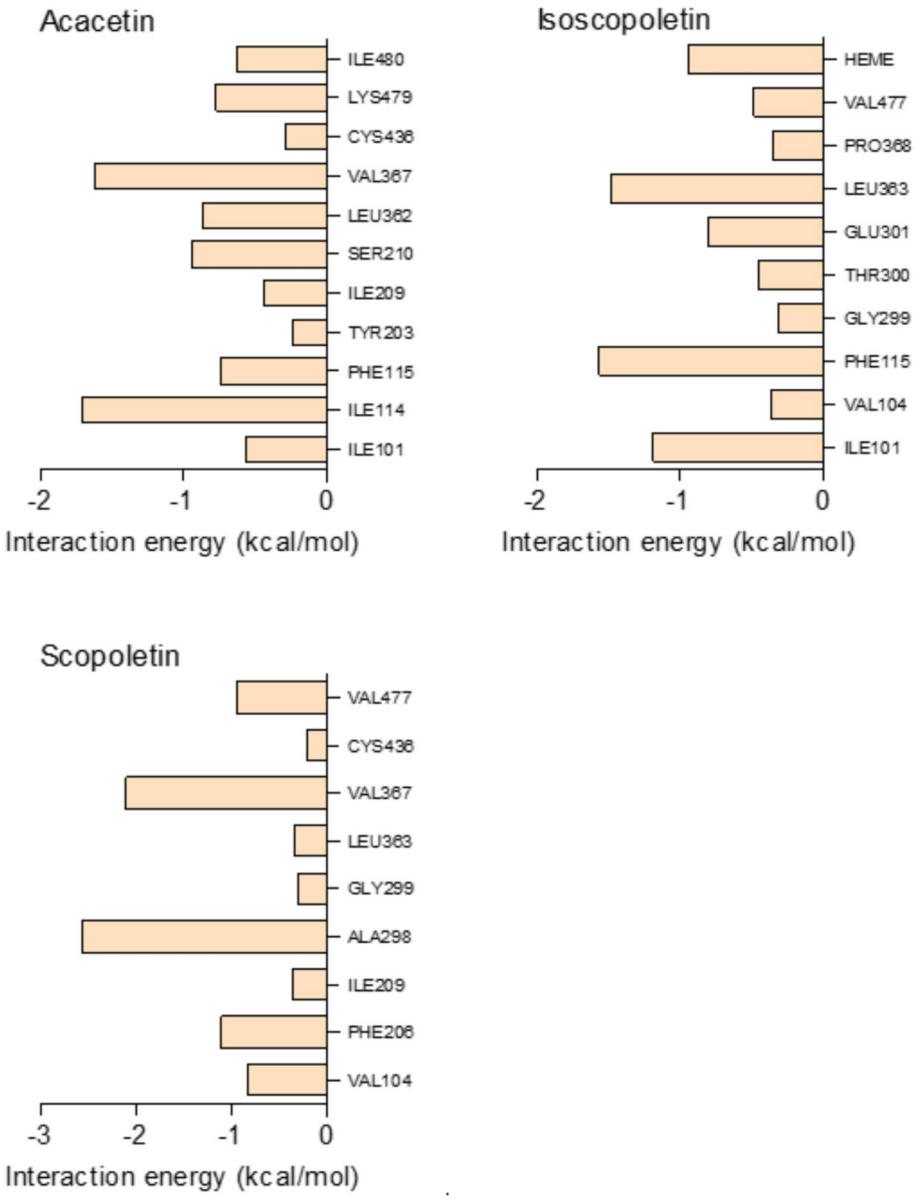

Fig. 4 Estimates of the interaction energies of acacetin, isoscopoletin, and scolopetin with active site residues of CYP2B6. Only productive energies more negative than – 0.2 kcal/mol are given

ligand stability and dynamic behaviour within the CYP2B6 binding site. Consequently, we acknowledge the lack of MD simulations as a constraint of our study. We recommend that future studies use MD simulations to provide a more comprehensive evaluation of ligand-CYP2B6 interactions, including stability metrics such as RMSD, RMSF, and hydrogen bond analyses, which will improve the structural credibility and predictive value of the results. Furthermore, we recommend that future studies include experimental validation, such as enzyme inhibition assays or binding studies, to confirm and complement the computational predictions and strengthen the overall conclusions.

4 Conclusion

In this study, we showed how in silico modelling could predict the binding of bioactive molecules from *Artemisia afra* aqueous extracts to CYP2B6, within limitations. These binding affinities were corroborated by literature. Utilising in silico molecular docking can predict the interplay between synthetic drugs and natural bioactive compounds, contributing to drug development, toxicity prediction, and personalised medicine strategies. The outcomes of the study also demonstrated that computational experiments can be conducted quicker at a minimal cost for screening. In silico studies can guide as a primary toward experimental validation studies. Results of the study also call for a consideration by healthcare authorities to draft health guidelines to guide in the clinical practice, the possibility of HDI that may arise. 75%–80% of the African population uses traditional medicine, and the use is on the rise in developed nations. Now, researchers in wet labs mainly focus on high-content phytochemical compounds while ignoring low-content bioactives. The combination of low and high-content compounds may have cumulative effects, and the advantage of the in silico molecular docking HDI screening approach is that it includes both low and high-content bioactive compounds.

Acknowledgements
We would like to thank Mr Chris van Niekerk of the NWU Botanical Gardens for sourcing and identifying the plants used in this study.

Author contributions
E.T. Nghilokwa: Conceptualization, data curation, formal analysis, investigation, visualization, and writing—original draft. J.P. Petzer: Data curation; Formal analysis; methodology; Resources: Software; Validation; Writing—Review and Editing. W. Pheiffer: Data curation; methodology; validation; visualization; supervision; writing—review and editing. I.Z. Hassan: Validation; Visualization; Supervision; Writing—Review and Editing. R.K. Hayeshi: Conceptualization, Supervision; Writing—Review and editing.

Funding
This research was funded by the North-West University.

Data availability
The manuscript contains all the data that underpins the findings of this study.

Declarations

Ethics and consent to participate
Not applicable.

Permissions to collect the plants/plant parts
All plant specimens were collected with permissions.

Plant guidelines
The plants used in the study *Artemesia afra* and *Catharanthus roseus* were acquired from the Botanical Garden of the North-West University (NWU), Potchefstroom, South Africa, and authenticated by the university's Botanist. After preparation, the herbarium voucher specimens bearing the specimen numbers PU0016058 and PUC0016057, respectively. The use of plants in the study complies with international, national, and/or institutional guidelines.

Consent for publication
Not applicable.

Competing interests
The authors declare no competing interests.

Received: 10 April 2025 / Accepted: 26 August 2025
Published online: 06 October 2025

References

1. Abera B. Medicinal plants used in traditional medicine by Oromo people, Ghimbi District, Southwest Ethiopia. J Ethnobiol Ethnomed. 2014. https://doi.org/10.1186/1746-4269-10-40.
2. Agbo MO, Uzor PF, Akazie-Nneji UN, Eze-Odurukwe CU, Ogbatue UB, Mbaoji EC. Antioxidant, total phenolic and flavonoid content of selected Nigerian medicinal plants. Dhaka Univ J Pharm Sci. 2015;14(1):35–41. https://doi.org/10.3329/dujps.v14i1.23733.

3. Ahad B, Shahri W, Rasool H, Reshi ZA, Rasool S, Hussain T. Medicinal plants and herbal drugs: an overview. Med Aromat Plants Healthcare Ind Appl. 2021. https://doi.org/10.1007/978-3-030-58975-2_1.
4. Aslam J, Siddiqui ZH, Zohra F. Catharanthus roseus (L.) G. Don . An important drug : Its applications and production Catharanthus roseus (L) G. Don. An important drug : it ' s applications and. International journal of comprehensive pharmacy, Pharmacie Globale (IJCP), 2010; Vol. 01, Issue 04, www.Pharmacie-Globale.Info
5. Bertrand H, Triballeau N. Virtual Screening Workflow Development Guided by the ROC Curve Approach. Application to High-Throughput Docking on Metabotropic Glutamate Receptor Subtype 4: Accepting the Uncertainty ? Receptor, 2005; 2534–2547.
6. Biswas P, Bibi S, Yousafi Q, Mehmood A, Saleem S, Ihsan A, et al. Study of MDM2 as prognostic biomarker in brain-LGG cancer and bioactive phytochemicals inhibit the p53-MDM2 pathway: a computational drug development approach. Molecules. 2023. https://doi.org/10.3390/molecules28072977.
7. Borse SP, Singh DP, Nivsarkar M. Understanding the relevance of herb–drug interaction studies with special focus on interplays: a prerequisite for integrative medicine. Porto Biomed J. 2019;4(2):e15. https://doi.org/10.1016/j.pbj.0000000000000015.
8. Chang TT, Chen KC, Chang KW, Chen HY, Tsai FJ, Sun MF, et al. In silico pharmacology suggests ginger extracts may reduce stroke risks. Mol Biosyst. 2011;7(9):2702–10. https://doi.org/10.1039/c1mb05228d.
9. Cole JC, Murray CW, Nissink JWM, Taylor RD, Taylor R. Comparing protein-ligand docking programs is difficult. Proteins. 2005;60(3):325–32. https://doi.org/10.1002/prot.20497.
10. Cox-georgian D, Ramadoss N, Dona C. Therapeutic and medicinal uses of terpenes. Med Plants. 2019. https://doi.org/10.1007/978-3-030-31269-5_15.
11. Cross JB, Thompson DC, Rai BK, Baber JC, Fan KY, Hu Y, et al. Comparison of several molecular docking programs: pose prediction and virtual screening accuracy. J Chem Inf Model. 2009;49(6):1455–74. https://doi.org/10.1021/ci900056c.
12. Dendy Darma M, Reza Faisal M, Budiman I, Herteno R, Utami JP, Abapihi B. In Silico Prediction of Indonesian Herbs Compounds as Covid-19 Supportive Therapy using Support Vector Machine. Proceedings—2021 4th International Conference on Computer and Informatics Engineering: IT-Based Digital Industrial Innovation for the Welfare of Society, IC2IE 2021, 62–67. https://doi.org/10.1109/IC2IE53219.2021.9649383
13. du Toit A, van der Kooy F. *Artemisia afra*, a controversial herbal remedy or a treasure trove of new drugs? J Ethnopharmacol. 2019. https://doi.org/10.1016/j.jep.2019.112127.
14. Ekins S, Wrighton SA. The role of CYP2B6 in human xenobiotic metabolism. Drug Metab Rev. 1999;31(3):719–54. https://doi.org/10.1081/DMR-100101942.
15. Ford GR, Niehaus A, Joubert F, Pepper MS. Pharmacogenetics of CYP2A6, CYP2B6, and UGT2B7 in the context of HIV treatments in African populations. J Pers Med. 2022. https://doi.org/10.3390/jpm12122013.
16. Gay SC, Shah MB, Talakad JC, Maekawa K, Roberts AG, Wilderman PR, et al. Crystal structure of a cytochrome P450 2B6 genetic variant in complex with the inhibitor 4-(4-chlorophenyl)imidazole at 2.0-Å resolution. Mol Pharmacol. 2010;77(4):529–38. https://doi.org/10.1124/mol.109.062570.
17. Gurib-fakim A. Medicinal plants: traditions of yesterday and drugs of tomorrow. Mol Aspects Med. 2006;27:1–93. https://doi.org/10.1016/j.mam.2005.07.008.
18. Hamilton MC, Heintz MM, Pfohl M, Marques E, Ford L, Slitt AL, et al. Increased toxicity and retention of perflourooctane sulfonate (PFOS) in humanized CYP2B6-Transgenic mice compared to Cyp2b-null mice is relieved by a high-fat diet (HFD). Food Chem Toxicol. 2021;152(January):112175. https://doi.org/10.1016/j.fct.2021.112175.
19. Hedrich WD, Hassan HE, Wang H. Insights into CYP2B6-mediated drug-drug interactions. Acta Pharm Sin B. 2016;6(5):413–25. https://doi.org/10.1016/j.apsb.2016.07.016.
20. Hirasawa Y, Kakizoe Y, Tougan T, Uchiyama N, Horii T, Morita H. Vincarostine A, a novel anti-malarial trimeric monoterpenoid indole alkaloid from *Catharanthus roseus*. J Nat Med. 2024. https://doi.org/10.1007/s11418-024-01795-1.
21. Ibrahim MAA, Abdeljawaad KAA, Roshdy E, Mohamed DEM, Ali TFS, Gabr GA, et al. In silico drug discovery of SIRT2 inhibitors from natural source as anticancer agents. Sci Rep. 2023. https://doi.org/10.1038/s41598-023-28226-7.
22. Izzo AA. Interactions between herbs and conventional drugs: overview of the clinical data. Med Princ Pract. 2012;21(5):404–28. https://doi.org/10.1159/000334488.
23. Kabubii ZN, Mbaria JM, Mbaabu M. Acute toxicity studies of Catharanthus roseus aqueous extract in male Wistar rats. Afr J Pharmacol Ther. 2015;4(4):130–4.
24. Kane NF. Effect of extracts of Artemisia afra collected from five different regions in Africa (Kenya , Burundi , Tanzania , South Africa and Senegal) on in vitro and in vivo cultures of Plasmodium Species. A Thesis Submitted to Pan African University Institute of Science, Technology and Innovation in Partial Fulfillment of the Requirement for the Award of the Degree of Doctor of Philosophy in Molecular Biology and Biotechnology of the Pan African University. 2019
25. Kane NF, Kyama MC, Nganga JK, Hassanali A, Diallo M, Kimani FT. Comparison of phytochemical profiles and antimalarial activities of *Artemisia afra* plant collected from five countries in Africa. South Afr J Bot. 2019;125:126–33. https://doi.org/10.1016/j.sajb.2019.07.001.
26. Kondža M, Mandić M, Ivančić I, Vladimir-Knežević S, Brizić I. Artemisia annua L. Extracts Irreversibly Inhibit the Activity of CYP2B6 and CYP3A4 Enzymes. Biomedicines. 2023;11:232.
27. Kumar RR. Phytochemical analysis of Catharanthus roseus plant extract and its antimicrobial activity main project view project degradation of plastics by microbes view project. Int J Pure App Biosci. 2015;3(2):162–72.
28. Kumar S, Bouic PJ, Rosenkranz B. Investigation of CYP2B6, 3A4 and β-esterase interactions of Withania somnifera (L.) dunal in human liver microsomes and HepG2 cells. J Ethnopharmacol. 2021. https://doi.org/10.1016/j.Jep.2020.113766.
29. Kumar S, Singh A, Kumar B, Singh B, Bahadur L, Lal M. Simultaneous quantitative determination of bioactive terpene indole alkaloids in ethanolic extracts of *Catharanthus roseus* (L.) G. Don by ultra high performance liquid chromatography–tandem mass spectrometry. J Pharm Biomed Anal. 2018;151:32–41. https://doi.org/10.1016/j.jpba.2017.12.040.
30. Lätti S, Niinivehmas S, Pentikäinen OT. Rocker: open source, easy-to-use tool for AUC and enrichment calculations and ROC visualization. J Cheminform. 2016;8(1):1–5. https://doi.org/10.1186/s13321-016-0158-y.
31. Li H, Zhang H, Zheng M, Luo J, Kang L, Liu X, et al. An effective docking strategy for virtual screening based on multi-objective optimization algorithm. BMC Bioinformatics. 2009;10:1–12. https://doi.org/10.1186/1471-2105-10-58.

32. Li X, Hu J, Wang B, Sheng L, Liu Z, Yang S, et al. Inhibitory effects of herbal constituents on P-glycoprotein *in vitro* and *in vivo*: herb-drug interactions mediated via P-gp. Toxicol Appl Pharmacol. 2014;275(2):163–75. https://doi.org/10.1016/j.taap.2013.12.015.
33. Liu J, Shah MB, Zhang Q, Stout CD, Halpert JR, Wilderman PR. Coumarin derivatives as substrate probes of mammalian cytochromes P450 2B4 and 2B6: assessing the importance of 7-Alkoxy chain length, halogen substitution, and non-active site mutations. Biochemistry. 2016;55(13):1997–2007. https://doi.org/10.1021/acs.biochem.5b01330.
34. Lovell T, Chen H, Lyne PD, Giordanetto F, Li J. On evaluating molecular-docking methods for pose prediction and enrichment factors. J Chem Inf Model. 2008;48(1):246–246. https://doi.org/10.1021/ci7003169.
35. Maddi EG. Traditional and herbal malaria treatment in Africa : an ethnobotanical analysis corresponding author : Journal of Coastal Life Medicine. 2023.
36. Mukonzo JK, Owen JS, Ogwal-Okeng J, Kuteesa RB, Nanzigu S, Sewankambo N, et al. Pharmacogenetic-based efavirenz dose modification: suggestions for an African population and the different CYP2B6 genotypes. PLoS ONE. 2014. https://doi.org/10.1371/journal.pone.0086919.
37. Mysinger MM, Carchia M, Irwin JJ, Shoichet BK. Directory of useful decoys, enhanced (DUD-E): better ligands and decoys for better benchmarking. J Med Chem. 2012;55(14):6582–94. https://doi.org/10.1021/jm300687e.
38. Nanjappan S, Paul D, Bolla L. Assessing herb-drug interactions of herbal products with therapeutic agents for metabolic diseases: analytical and regulatory perspectives. In: Studies in natural products chemistry, vol. 59. 1st ed. Amsterdam: Elsevier B.V; 2018.
39. Ngaimisi E, Habtewold A, Minzi O, Makonnen E, Mugusi S, Amogne W, et al. Importance of ethnicity, CYP2B6 and ABCB1 genotype for efavirenz pharmacokinetics and treatment outcomes: a parallel-group prospective cohort study in two sub-Saharan Africa populations. PLoS ONE. 2013. https://doi.org/10.1371/journal.pone.0067946.
40. Enoche OF, Sekine S, Yoshihisa Shitara TH. Pharmacokinetic Herb-drug interactions: insight into mechanisms and consequences. Eur J Drug Metab Pharmacokinet. 2016;41(2):93–108. https://doi.org/10.1007/s13318-015-0296-z.
41. Olivier D, van der Kooy F, Gerber M. Geographical and seasonal phytochemical variation of *Artemisia afra* Jacq. ex Willd. Phytochem Anal. 2023;34(2):175–85. https://doi.org/10.1002/pca.3191.
42. Pham HNT, Vuong QV, Bowyer MC, Scarlett CJ. Phytochemicals derived from *Catharanthus roseus* and their health benefits. Technologies. 2020;8(4):80. https://doi.org/10.3390/technologies8040080.
43. PrabhaLahare R, Yadav HS, Dashahre AK, Kumar Bisen Y. An updated review on phytochemical and pharmacological properties of catharanthus rosea. Saudi J Med Pharm Sci. 2020;6(12):759–66. https://doi.org/10.36348/sjmps.2020.v06i12.007.
44. Sama-ae I, Pattaranggoon NC, Tedasen A. In silico prediction of antifungal compounds from natural sources towards Lanosterol 14-alpha demethylase (CYP51) using molecular docking and molecular dynamic simulation. J Mol Graph Model. 2023. https://doi.org/10.1016/j.jmgm.2023.108435.
45. Senra MVX. In silico characterization of cysteine-stabilized αβ defensins from neglected unicellular microeukaryotes. BMC Microbiol. 2023. https://doi.org/10.1186/s12866-023-02817-w.
46. Shah MB, Liu J, Zhang Q, Stout CD, Halpert JR. Halogen-π interactions in the cytochrome P450 active site: structural insights into human CYP2B6 substrate selectivity. ACS Chem Biol. 2017;12(5):1204–10. https://doi.org/10.1021/acschembio.7b00056.
47. Shah MB, Pascual J, Zhang Q, Stout CD, Halpert JR. Structures of cytochrome P450 2B6 bound to 4-benzyl pyridine and 4-(4-nitrobenzyl) pyridine: insight into inhibitor binding and rearrangement of active site side chains. Mol Pharmacol. 2011;80(6):1047–55. https://doi.org/10.1124/mol.111.074427.
48. Shaw M, Petzer A, Petzer JP, Cloete TT. The pterin binding site of dihydropteroate synthase (DHPS): In silico screening and in vitro antibacterial activity of existing drugs. Results Chem. 2023. https://doi.org/10.1016/j.rechem.2023.100863.
49. Shah MB, Wilderman PR, Liu J, Jang HH, Zhang Q, Stout CD, Halpert JR. Structural and biophysical characterization of human cytochromes P450 2B6 and 2A6 bound to volatile hydrocarbons: analysis and comparison. Mol Pharmacol. 2015;87(4):649–59. https://doi.org/10.1124/mol.114.097014.
50. Shah MB, Zhang Q, Halpert JR. Crystal structure of CYP2B6 in complex with an efavirenz analog. Int J Mol Sci. 2018. https://doi.org/10.3390/ijms19041025.
51. Singh H, Bharadvaja N. Treasuring the computational approach in medicinal plant research. Prog Biophys Mol Biol. 2021;164:19–32. https://doi.org/10.1016/j.pbiomolbio.2021.05.004.
52. Teng Z, Zhang Y, Dai Q, Wu C, Li D. Constructing discriminative feature space for LncRNA–protein interaction based on deep autoencoder and marginal fisher analysis. Comput Biol Med. 2023. https://doi.org/10.1016/j.compbiomed.2023.106711.
53. Turpeinen M, Nieminen R, Juntunen T, Taavitsainen P, Raunio H, Pelkonen O. Selective inhibition of CYP2B6-catalyzed bupropion hydroxylation in human liver microsomes *in vitro*. Drug Metab Dispos. 2004;32(6):626–31. https://doi.org/10.1124/dmd.32.6.626.
54. Turpeinen M, Raunio H, Pelkonen O. The functional role of CYP2B6 in human drug metabolism: substrates and inhibitors in vitro, in vivo and in silico. Curr Drug Metab. 2006;7(7):705–14. https://doi.org/10.2174/138920006778520633.
55. Turpeinen M, Zanger UM. Cytochrome P450 2B6: function, genetics, and clinical relevance. Drug Metab Drug Interact. 2012;27(4):185–97. https://doi.org/10.1515/dmdi-2012-0027.
56. Van Vuuren SF, Motlhatlego KE, Netshia V, et al. Traditionally used polyherbals in a southern African therapeutic context. J Ethnopharmacol. 2022;288:114977. https://doi.org/10.1016/j.jep.2022.114977.
57. Venkateswarulu TC, Vajiha KS, Mikkili I, Angelina J, John Babu D, Peele KA. In silico study on evaluation of corosolic acid of Lagerstroemia speciosa against Alzheimer's disease. Arab Gulf J Sci Res. 2023;41(2):175–82. https://doi.org/10.1108/AGJSR-04-2022-0039.
58. Viljoen A, Chen W, Mulaudzi N, Kamatou G, Sandasi M. Artemisia afra. Phytochemical Profiling of Commercially Important South African Plants, 2022; 39–54. https://doi.org/10.1016/b978-0-12-823779-3.00004-7
59. Vogel D, Loots E, Oladimeji O, Gouws C, van der Kooy F. The anti-neoplastic activity of *Artemisia afra* in breast cancer cell lines. South Afr J Bot. 2023;157:115–21. https://doi.org/10.1016/j.sajb.2023.03.049.
60. Wang L, Hai Y, Huang N, Gao X, Liu W, He X. Human cytochrome P450 enzyme inhibition profile of three flavonoids isolated from: *Psoralea corylifolia*: in silico predictions and experimental validation. New J Chem. 2018;42(13):10922–34. https://doi.org/10.1039/c7nj00884h.

61. Wei BQ, Baase WA, Weaver LH, Matthews BW, Shoichet BK. A model binding site for testing scoring functions in molecular docking: this work is dedicated to the memory of Andy Morton (1964–1997). J Mol Biol. 2002;322(2):339–55. https://doi.org/10.1016/S0022-2836(02)00777-5.
62. WHO. (2016). African Region Communicable Diseases Cluster Annual Report 2016. *Communicable Disease Cluster, Annual Report*, 1–48. AFRO CDS Annual Report 2016 web version_1.pdf https://www.afro.who.int/sites/default/files/2017-11/WHO
63. WHO. World Malaria Report 2020. In WHO. 2020; Vol. 73, Issue 1. https://www.who.int/teams/global-malaria-programme/reports/world-malaria-report-2020
64. WHO. WHO Guidelines for Malaria—3 June 2022. WHO, 2022. http://apps.who.int/bookorders. https://www.who.int/Teams/Global-Malaria-Programme
65. Zanger UM, Klein K. Pharmacogenetics of cytochrome P450 2B6 (CYP2B6): advances on polymorphisms, mechanisms, and clinical relevance. Front Genet. 2013;4:1–12. https://doi.org/10.3389/fgene.2013.00024.
66. Zanger UM, Klein K, Saussele T, Blievernicht J, Hofmann MH, Schwab M. Polymorphic CYP2B6: molecular mechanisms and emerging clinical significance. Pharmacogenomics. 2007;8(7):743–59. https://doi.org/10.2217/14622416.8.7.743.
67. Zhang Y, Chen R, Zhang D, Qi S, Liu Y. Metabolite interactions between host and microbiota during health and disease: which feeds the other? Biomed Pharmacother. 2023. https://doi.org/10.1016/j.biopha.2023.114295.

Publisher's Note